Variation of Hg concentration and accumulation in the soil of maritime pine plantations along a coast-inland transect in SW Europe

Melissa Méndez-López [a,b,*], Cristina Eimil-Fraga [c], Flora Alonso-Vega [a,b], Roque Rodríguez-Soalleiro [c], Esperanza Álvarez-Rodríguez [d], Manuel Arias-Estévez [a,b], Juan Carlos Nóvoa-Muñoz [a,b]

[a] *Universidade de Vigo, Departamento de Bioloxía Vexetal e Ciencia do Solo, Área de Edafoloxía e Química Agrícola, Facultade de Ciencias. As Lagoas S/n, 32004, Ourense, Spain*
[b] *Campus da Auga, Universidade de Vigo, Laboratorio de Tecnoloxía e Diagnose Ambiental. Rúa Canella da Costa da Vela 12, 32004, Ourense, Spain*
[c] *Unidad de Gestión Ambiental y Forestal Sostenible, Escuela Politécnica Superior de Ingeniería, Universidade de Santiago de Compostela. Rúa Benigno Ledo S/n, 27002, Lugo, Spain*
[d] *Departamento de Edafología y Química Agrícola, Escuela Politécnica Superior de Ingeniería, Universidade de Santiago de Compostela, Rúa Benigno Ledo S/n, 27002, Lugo, Spain*

A R T I C L E I N F O

A B S T R A C T

Climatic conditions have been shown as a major driver of the fate of Hg in forest ecosystems at a global scale, but less is known about climatic effects at shorter scales. This study assesses whether the concentration and pools of Hg in soils collected from seventeen *Pinus pinaster* stands describing a coastal-inland transect in SW Europe vary along a regional climatic gradient. In each stand, samples of the organic subhorizons (OL, OF + OH) and the mineral soil (up to 40 cm) were collected and some general physico-chemical properties and total Hg (THg) were analyzed. Total Hg was significantly higher in the OF + OH than in the OL subhorizons (98 and 38 µg kg^{-1}, respectively), favored by a greater organic matter humification in the former. In the mineral soil, mean THg values decreased with depth, ranging from 96 µg kg^{-1} in the 0–5 cm layers to 54 µg kg^{-1} in the deepest layers (30–40 cm), respectively. The average Hg pool (PHg) was 0.30 mg m^{-2} in the organic horizons (92% accumulated in the OF + OH subhorizons), and 27.4 mg m^{-2} in the mineral soil. Changes in climatic factors, mainly precipitation, along the coast-inland transect resulted in a remarkable variation of THg in the OL subhorizons, consistent with their role as the first receiver of atmospheric Hg inputs. The high precipitation rate and the occurrence of fogs in coastal areas characterized by the oceanic influence would explain the higher THg found in the uppermost soil layers of pine stands located close to the coastline. The regional climate is key to the fate of mercury in forest ecosystems by influencing the plant growth and subsequent atmospheric Hg uptake, the atmospheric Hg transference to the soil surface (wet and dry deposition and litterfall) and the dynamics that determine net Hg accumulation in the forest floor.

1. Introduction

Mercury (Hg) is considered a global pollutant because of its ability to be mobilized over long distances through the atmosphere before its deposition and due to its high capacity to bioaccumulate, causing diseases in living organisms (UN Environment, 2019). Among the terrestrial biomes, forests constitute a major sink of atmospheric Hg (Bishop et al., 2020; Obrist et al., 2021). This is because tree canopies are

actively involved in the scavenging of atmospheric Hg and its accumulation in the aboveground biomass (Zhou et al., 2021), being subsequently deposited to the forest floor through litterfall (Wang et al., 2016). Moreover, Hg may also reach the uppermost layers of forest soils after being washed away from the surface of plant tissues by throughfall and stemflow, or deposited by precipitation through wet deposition (Louis et al., 2001; Wright et al., 2016). As consequence, soils are another essential component in the biogeochemical Hg cycle in forests,

---

being considered as net sinks of Hg and hindering its mobilization to other environmental compartments (Grigal, 2003).

Mercury storage on vegetation and soil in forest ecosystems is highly influenced by the type of vegetation (Obrist et al., 2012; Zhou et al., 2017; Wang et al., 2019a; Gruba et al., 2019; Méndez-López et al., 2022a). Thus, it was shown that Hg accumulation in conifer needles may extent up to three years without evidence of saturation and their accumulation rates were related to the specific leaf area (Pleijel et al., 2021). Moreover, once deposited on the forest floor, Hg retention in the organic horizons is favored by the high lignin and low nitrogen content of needles, which delays litter decomposition and facilitates Hg accumulation (Obrist et al., 2009; Pokharel and Obrist, 2011).

Although vegetation is a major driver of Hg accumulation in forest soils, Hg dynamics in the air-vegetation-soil transfer cycle were reported to be strongly linked to climatic features both at local (Stankwitz et al., 2012), regional (Richardson et al., 2013; Obrist et al., 2016; Zhang et al., 2020) and global scales (Wang et al., 2019a). Thus, it has been demonstrated that coastal environments, compared to inland areas, are potential receivers of gaseous oxidized Hg (GOM) bound to sea salt aerosols (Malcolm et al., 2009), which are efficiently removed from the atmosphere in maritime areas by precipitation and fog (Tsyro et al., 2011). Zhang et al. (2020) reported that the wet deposition of Hg in Asia is strongly influenced by the precipitation associated with the monsoon season. Recently, Méndez-López et al. (2022b) found that humidity and precipitation were responsible for the different Hg concentrations in needles of *Pinus pinaster* plantations located along a transition area between the Atlantic and Mediterranean biogeographical regions in the NW Iberian Peninsula. However, the incidence of fog in coastal areas is not only relevant in mobilizing GOM to nearshore environments (Cheng et al., 2013; Coale et al., 2018), but also in enhancing the growth and activity of trees (Fischer et al., 2016) and the metabolism of microorganisms involved in soil organic matter recycling (Carbone et al., 2011, 2013).

The ability of forest ecosystems to accumulate Hg is not only affected by the geographical location, but also by direct and indirect human activities (Obrist et al., 2018). Processes that may modify the biogeochemical cycle of Hg in forest ecosystems include tree clearcutting (Porvari et al., 2003; Eckley et al., 2018), frequency and severity of wildfires (Campos et al., 2015; Kumar et al., 2018), extreme weather events (Yuan et al., 2022) and variations in plant productivity (Jiskra et al., 2018). This is an issue of concern, as areas from the NW Iberian Peninsula afforested with maritime pine (*P. pinaster*) have been recently catalogued as highly prone to be affected by wildfires (de Diego et al., 2021), with subsequent risks of Hg mobilization and impact on the biota of soil and freshwater ecosystems.

The present study assesses if the variation in climatic factors, such as rainfall, may influence the concentration and accumulation of Hg in different soil layers of *P. pinaster* stands at a regional scale. For this purpose, a coast-inland transect was established in Galicia (NW Iberian Peninsula), covering a transitional area between the Eurosiberian and the Mediterranean biogeographical regions. The results are expected to improve the accuracy of global models on the fate of Hg in terrestrial ecosystems including variations induced by regional climatic conditions. Total Hg contents and storage (pools) were quantified in the organic and mineral soil layers of seventeen *P. pinaster* stands, assessing the influence of several factors such as distance to the coastline, altitude, precipitation and different physicochemical soil properties. New empirical data on Hg storage in soils would help to redefine previous estimates from large-scale surveys in Europe. Data will also serve to warn stakeholders about the risk of soil Hg mobilization during forestry practices, raising awareness about the need to improve timber management and harvesting practices.

2. Material and methods

2.1. Study area

The study was carried out in seventeen even-aged *Pinus pinaster* (Ait.) plantations (23–25 years old) distributed along a coast-inland transect in Galicia (NW Iberian Peninsula), which spans along a west-to-east strip of approximately 150 km length from the coastline (Fig. 1, Table S1). The economic activity in this territory is mainly based on the primary sector, with aquaculture and fishing as the main activities in the coastal areas, and with agriculture and livestock gaining relevance as we move away from the coastline. Activities related to forestry are also relevant throughout all the territory. The secondary sector in Galicia is supported by renewable energy production, automobile manufacturing, building and textile industry.

Some forestry characteristics of the studied pine stands are shown in Table S2. In general, the study area is influenced by an oceanic climate with prevailing westerly and south-westerly winds and with mean annual temperatures varying from 14 °C in the coastal areas to 12 °C inland. Along the coastal-inland transect, which reflects a transition between the Eurosiberian and the Mediterranean biogeographical regions, cloudiness, fog drip (from 100 to 30 days per year) and mean annual rainfall (from 2200 to 800 mm) show a gradual decrease as we move away from the Atlantic Ocean coast (Martínez-Cortizas et al., 1999; Martí-Ezpeleta et al., 2018).

The forest vegetation in the study stands is dominated by maritime pine (*Pinus pinaster*, Ait.), while the understory is composed of fern (*Pteridium aquilinum*), blackberry (*Rubus ulmifolius*) and mixed shrubs (*Calluna vulgaris, Erica* sp., *Ulex* sp.). The lithology across the study area is diverse comprising granitic rocks, schist and slate as main soil parent materials where selected pine stands were located (Table S1).

2.2. Soil sampling, preparation and physico-chemical characterization

The seventeen *Pinus pinaster* stands selected for this study were located far away from diffuse and point anthropogenic sources of Hg emissions (Fig. 1). In each stand, three representative plots of 15 × 15 m were established keeping a distance of at least 30 m from forest tracks. In each plot, an area without visible evidence of soil perturbation was selected for soil sampling. The organic horizon was sampled using a 50 × 50 cm wood square frame placed on the soil and held in place by stainless steel anchoring stakes driven into the outer edges. Organic horizon samples were collected differentiating, according to Zanella et al. (2018), an OL subhorizon consisting of undecomposed and distinguishable litter remains and the combination of the OF and OH subhorizons (OF + OH), which includes partially decomposed and indistinguishable litter. During sampling, we made note of the depth of each subhorizon at the corners of the square frame to subsequently calculate the bulk density. At the same location and after removing the organic subhorizons, mineral soil samples were collected at different depth intervals: 0–5, 5–10, 10–20, 20–30 and 30–40 cm. A stainless steel ring (100 cm^3) was inserted in each mineral soil layer to determine the bulk density. Nitrile free-powder gloves, a garden trowel and a handsaw were used during collection and soil samples were doubled-bagged and kept in a portable fridge for transportation to the laboratory. Moreover, a sample of unweathered soil parent material (representative of the local lithology) was collected from each stand.

Once in the laboratory, stones and large wood debris were removed from soil samples, which were then oven-dried at 40 °C. Then, organic horizon samples were weighed and crushed to a particle size <4 mm, whereas mineral soil samples were sieved to <2 mm. An aliquot of all soil samples (organic and mineral) was ground in an agate mortar for subsequent analyses, while a subsample of the organic horizons was oven-dried at 105 °C (48 h) to determine the dry mass at a constant weight. For each mineral soil layer, an equal amount of sieved soil from each of the three plots was mixed using a stainless steel riffle splitter to
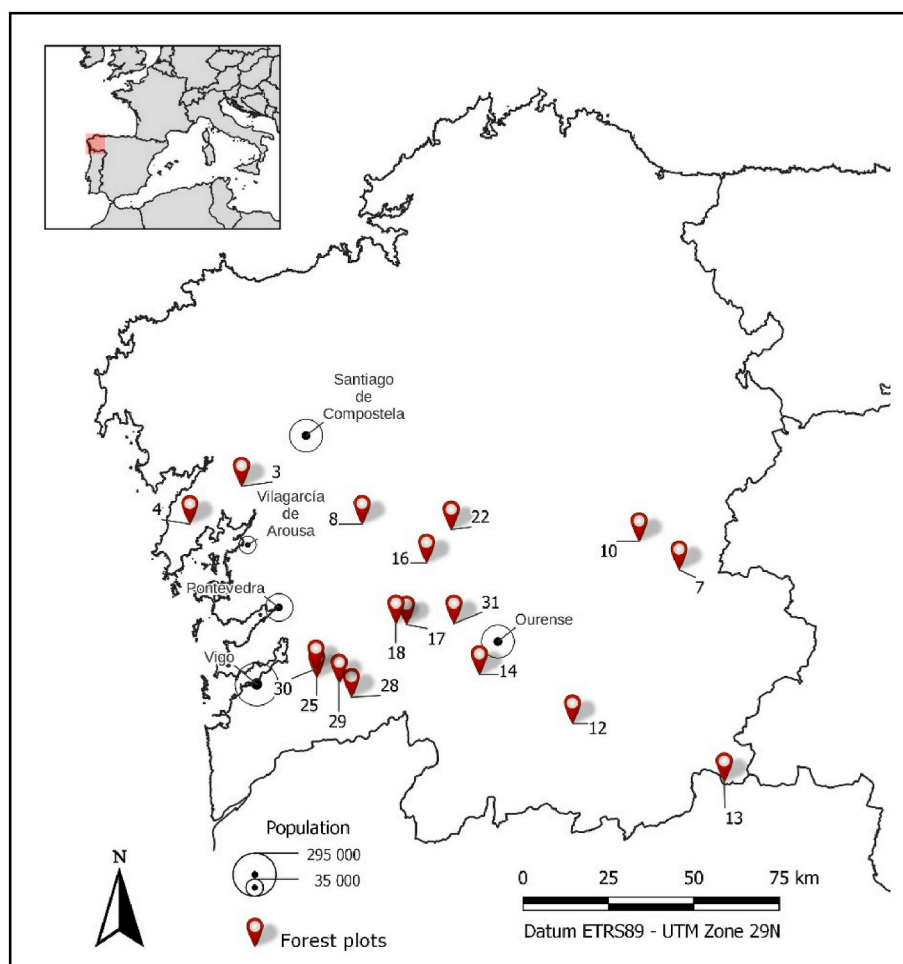
Fig. 1. Location of the study area (Galicia, the NW Iberian Peninsula) in SW Europe and distribution of the 17 *Pinus pinaster* stands (red labels) along the coastal-inland transect. The major cities of the coast-inland transect assessed and their population are also shown in the figure.

obtain a composite sample per stand. The bulk density of the organic horizons was estimated as a function of the sampling area (0.25 m^2), the dry soil mass and the thickness of each organic layer, and for the mineral soil layers, it was based on the dry mass of the soil contained in the stainless steel rings of 100 cm^3. Lithological samples were cleaned with distilled water to remove soil debris and dried at room temperature, then crushed into smaller pieces and, finally, ground in an agate mechanical mortar. During sample processing, the equipment used (grinders, sieves, mortar) was properly cleaned with diluted HCl and distilled water to avoid cross-contamination among samples.

The chemical characterization of the organic horizons (n = 102) included pH in distilled water (pH$_w$) and saline solution (pH$_k$), total C and N contents and the sum of exchangeable base cations (Na$^+$, K$^+$, Ca^{2+}, Mg^{2+}). In the mineral soils samples, pH (in water and saline solution), the sum of exchangeable base cations and Fe and Al distribution were performed on the composite samples obtained for each depth interval and stand (n = 82). For Al and Fe fractionation in mineral soil samples, a 0.1 M Na-pyrophosphate solution was used to determine total metal (Al, Fe)-humus complexes (Al$_p$, Fe$_p$). The 0.2 M ammonium oxalate-oxalic acid solution buffered at pH 3 was used to extract metal (Al, Fe)-humus complexes plus inorganic non-crystalline Al and Fe oxyhydroxides (Al$_o$, Fe$_o$). Finally, total secondary Al and Fe compounds, i.e. total free Al and Fe, were determined using 0.5 M NaOH solution (Al$_n$) and Na-dithionite-citrate solution (Fe$_d$), respectively. Moreover, particle size distribution was determined in composite samples of mineral soil corresponding to two depth intervals (5–10 and 20–30 cm), whereas total C and N contents were analyzed in all individual mineral

soil samples (n = 241). Additional information about the procedures for physico-chemical characterization of soil samples is available in Text S1 (Supplementary Material).

2.3. Total mercury analysis

The concentration of total Hg (THg) was analyzed in the individual ground samples of organic horizons (n = 102), mineral soil (n = 241) and parent material (n = 17). For this purpose, around 100 mg of each soil sample were weighed and measured in a tri-cell DMA-80 (Milestone), whose methodology is based on thermic decomposition, amalgamation and atomic absorption spectrometry (US EPA 7473). For greater precision in the analyses of total Hg content, all samples were analyzed in duplicate provided that the coefficient of variation between replicates was less than 10%. Otherwise, the measurement was repeated until such condition was achieved. For quality assurance and control (QA/QC), standard reference materials GBW 07402 (soil; 15 ± 3 µg kg^{-1}) and BCR 142 R (soil; 67 ± 11 µg kg^{-1}) were measured at the beginning and end of each analytical run and every twelve samples, obtaining mean recoveries of 91 and 111%, respectively. The limit of detection (LOD) was 0.43 µg kg^{-1} considering an average mass sample of 100 mg of soil.

The estimation of the total Hg pool (PHg) for each organic horizon and mineral soil layers was based on thickness, bulk density and total Hg concentration.

2.4. Statistical analysis of data

All statistical analyses were performed with IBM SPSS Statistics (25th version) by applying non-parametrical tests. The influence of the type of organic subhorizon and the mineral soil layer on Hg concentrations and pools was checked by applying a Kruskal-Wallis test (H). Relationships among parameters relative to Hg (THg and PHg) and soil physico-chemical characteristics, distance to the coastline (retrieved from Méndez-López et al., 2022b) and mean annual precipitation between 2015 and 2019 (Table S1) were established with the Spearman rank correlation test (ρ). Statistical significance was considered when p < 0.05. Data on mean annual precipitation were acquired from weather stations located close to the pine stands, which belong to Meteogalicia (Meteogalicia.gal, 2022), a public agency for the regional weather forecast in the NW Iberian Peninsula.

3. Results and discussion

3.1. General soil characterization

In most of the soils, the sand fraction (fine + coarse sand) dominated the particle size distribution with values in the range of 40–80%, resulting in a predominance of the sandy loam texture (Table S3), although finer textures (loam) were found in soils developed from slates.

Regarding soil chemical properties (Table 1), mean values of soil pH in distilled water (pH_w) varied from 4.1 to 4.7, being somewhat lower (range 3.1–3.9) when pH was measured in saline solution (pH_k). Both pH_w and pH_k showed a raising trend towards deeper mineral soil layers, whose values were comparable to the ranges (3.9–5.3 and 3.7–4.4, respectively) reported in pine forest soils from different areas of the Iberian Peninsula (Álvarez et al., 2002; Eimil-Fraga et al., 2015a; López-Marcos et al., 2018). The strong acidity in the studied soils is common in coniferous forests, due to a slower organic matter decomposition rate, greater generation of organic acids and lower release of exchangeable base cations (Hagen-Thorn et al., 2004). The highest total C and N contents were found in the organic horizons (>405 and >8 g kg^{-1}, respectively), decreasing with depth in the mineral soil where mean values ranges were 47–120 g kg^{-1} for organic C and 3–6 g kg^{-1} for total N. These data of total organic C and N were similar to those published for pine forest soils in the surroundings of the study area (Álvarez et al., 2002; Eimil-Fraga et al., 2015a). Mean values of the C/N ratio in the mineral soil scarcely varied with depth (range 17–20), but reached up to 73 in the OL subhorizon. The C/N ratios found in the studied soils were in the range (15–105) reported for forests soils dominated by *Pinus*

pinaster in the Iberian Peninsula (Álvarez et al., 2002; Fonseca and De Figueiredo, 2018; López-Marcos et al., 2018). The decrease in total C and N contents and C/N ratio with soil depth is a common feature in forest soils, and the lower mean C/N ratio in the OF + OH compared to the OL subhorizons indicates a considerable transformation of organic matter in the former (Cools et al., 2014; Herrero et al., 2016). The sum of exchangeable base cations (SB) was dominated by Ca and Mg in the organic horizons (Table S4) and showed mean values (15–18 cmol$_c$ kg^{-1}) up to two orders of magnitude higher than in the mineral soil (<1.6 cmol$_c$ kg^{-1}). Aluminium occupied most of the binding sites of the cation exchange complex in the mineral soil layers with a range of Al saturation of 77–84% (Table S4), being similar to those (64–90%) reported by Álvarez et al. (2002) in pine forest soils.

The fractionation of Al in the mineral soil was dominated by Al-humus complexes (Al_p), accounting for 55% of the total secondary Al compounds (Al_n). The mean values of Al_p were in the range 3.2–6.2 g kg^{-1} (Fig. S1), similar to the interval 2.3–6.5 g kg^{-1} reported by Álvarez et al. (2002) in pine forest soils. The presence of Al-humus complexes increased with soil depth due to greater humification of soil organic matter (as indicated by the C/N ratio), which led to stronger interactions between Al and organic C compounds (Kaal et al., 2008; Eimil-Fraga et al., 2015a). Crystalline Al compounds (Al_c, estimated as Al_n-Al_o), the second in abundance, showed mean values varying from 1.8 to 5.4 g kg^{-1} (Fig. S1). The increasing trend of Al_c content with soil depth may be a consequence of weathering of primary soil minerals, as well as the control of Al solubility by soil pH and secondary Al minerals (Ferro-Vázquez et al., 2014). The inorganic non-crystalline Al compounds (Al_{ia}, estimated as Al_o-Al_p) showed mean values below 1.4 g kg^{-1} (Fig. S1).

Crystalline Fe oxyhydroxides (Fe_c, estimated as Fe_d-Fe_o) accounted for up to 65% of the total reactive Fe compounds in the studied soils, showing mean values in the range of 9.2–11.3 g kg^{-1} (Fig. S1). The predominance of crystalline Fe compounds is common in the deeper soil layers of acid forest soils from temperate areas (Ferro-Vázquez et al., 2014). The Fe-humus complexes (Fe_p) contributed to 28% of total reactive Fe compounds (averages 3.3–5.1 g kg^{-1}, Fig. S1) and were reported to participate in the stabilization of Al-humus complexes and, consequently, organic C accumulation in acid soils (Ferro-Vázquez et al., 2014).

3.2. Mercury concentrations and pools in pine forest soils

The concentration of total Hg (THg) in the OL subhorizons showed values in the range of 26–78 µg kg^{-1} (average 38 µg kg^{-1}, Fig. 2). Considering that OL subhorizons are mainly comprised of pine needles, the values of THg found in the OL subhorizon are consistent with the range (16–51 µg kg^{-1}) obtained in old pine needles (3 and 4 years old) collected from stands distributed along the same area of the present study (Méndez-López et al., 2022b). Tree leaves and needles constitute the plant tissue that uptake atmospheric Hg more actively during their lifetime and they are directly involved in Hg transference to soil surface through litterfall (Wang et al., 2019a; Zhou et al., 2021).

The concentration of total Hg in the OF + OH subhorizons (98 ± 27 µg kg^{-1}) was significantly higher than in the OL layers (H = 72.251; p = 0.000; n = 100), ranging from 53 to 182 µg kg^{-1} (Fig. 2). The increase of THg the more decomposed the organic matter is, i.e. lower C/N ratio, justifies greater THg values in OF + OH than OL subhorizons. This was attributed to a prevalent loss of organic carbon over Hg during organic matter decomposition (Pokharel and Obrist, 2011), as well as greater availability of binding sites in the more humified OF + OH layers to capture Hg (Demers et al., 2007). The relationship observed between Hg/C and C/N ratios for organic horizons (Fig. 3) is in agreement with that reported in other studies (Obrist et al., 2011; Gómez-Armesto et al., 2020a) and supports the preferential Hg retention observed in the OF + OH subhorizons.

Total Hg concentrations in the complete O horizons (OL and OF +

Table 1
Mean values and standard deviation ($\pm$) of selected physico-chemical properties of soils.

Soil layer	BD[a] g cm^{-3}	pH_w	pH_k	C g kg^{-1}	N g kg^{-1}	C/N	SB[a] cmol$_c$ kg^{-1}
OL	0.04 ± 0.02	4.5 ± 0.3	3.7 ± 0.3	498 ± 12	7.6 ± 2.7	73 ± 22	17.6 ± 3.4
OF + OH	0.08 ± 0.04	4.5 ± 0.2	3.5 ± 0.2	405 ± 61	12.6 ± 2.9	34 ± 7	15.2 ± 4.3
0–5	0.58 ± 0.14	4.1 ± 0.3	3.1 ± 0.3	120 ± 38	6.3 ± 2.4	20 ± 3	1.6 ± 0.7
5–10	0.77 ± 0.17	4.2 ± 0.2	3.4 ± 0.3	86 ± 31	4.9 ± 2.2	19 ± 4	0.9 ± 0.3
10–20	0.84 ± 0.16	4.4 ± 0.3	3.6 ± 0.2	72 ± 26	4.1 ± 1.8	18 ± 3	0.7 ± 0.2
20–30	0.95 ± 0.20	4.6 ± 0.2	3.8 ± 0.2	55 ± 26	3.2 ± 1.7	17 ± 3	0.6 ± 0.2
30–40	1.00 ± 0.18	4.7 ± 0.2	3.9 ± 0.2	47 ± 25	2.9 ± 1.7	17 ± 3	0.6 ± 0.2

[a] BD is the bulk density of the soil layer and SB means the sum of exchangeable base cations (Ca + Mg + K + Na).
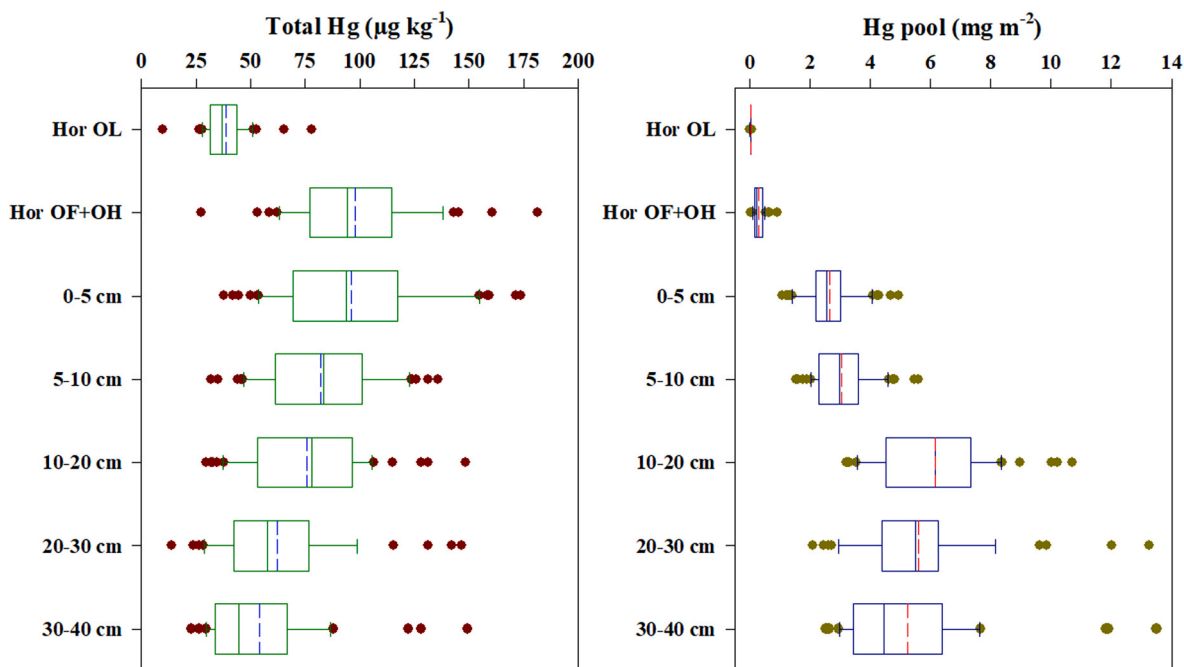
Fig. 2. Box and whisker plot of total Hg concentration (THg) and pool (PHg) in the different organic subhorizons and mineral soil layers of the seventeen *Pinus pinaster* stands. The box shows the interquartile range (from 25th to 75th percentiles), the solid line in the middle of the box marks the median value (50th percentile) and the dashed line marks the average value. The whiskers extend from the minimum to the maximum value observed. The points outside the box are outliers.
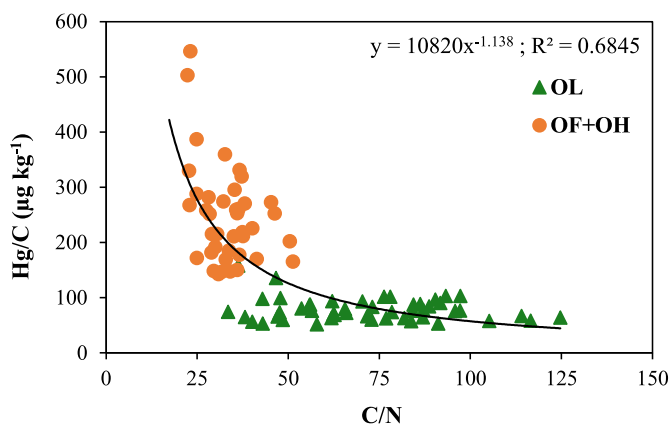

Fig. 3. Regression between Hg/C and C/N ratios in the OL and OF + OH subhorizons.

OH) correlated with total C ($\rho = -0.758$; $p = 0.000$; $n = 102$), total N ($\rho = 0.721$; $p = 0.000$; $n = 102$) and the C/N ratio ($\rho = -0.807$; $p = 0.000$; $n = 102$). Similar relationships were found in previous studies (Obrist et al., 2009; Juillerat et al., 2012; Navrátil et al., 2014; Richardson and Friedland, 2015; Blackwell and Driscoll, 2015; Méndez-López et al., 2022b), which arise from the strong affinity between Hg and soil organic matter (Skyllberg, 2010). Negative correlations between THg and total organic C and C/N ratio suggest that interactions between Hg and organic matter depend more on organic matter quality than quantity (Burns et al., 2014; Richardson and Friedland, 2015; Méndez-López et al., 2022b).

In general, most of the organic subhorizons (82% of samples) showed THg values below 100 µg kg^{-1}, which can be considered a background Hg level (Gustin et al., 2008), confirming that the study area is not significantly influenced by anthropogenic point sources of Hg emission. Our values of THg in the organic horizons are comparable to those found in soils under *Pinus* species in different areas worldwide, such as NE Portugal (65–110 µg kg^{-1}; Méndez-López et al., 2022a), China (54–210

µg kg^{-1}; Zhou et al., 2017; Du et al., 2019), the USA (22–134 µg kg^{-1}; Obrist et al., 2009) or Poland (average 120 µg kg^{-1}; Gruba et al., 2019).

In the mineral soil, mean values of THg diminished with depth from 96 ± 35 µg kg^{-1} in the uppermost mineral layer (0–5 cm) to 54 ± 28 µg kg^{-1} in the 30–40 cm layer (Fig. 2), showing significant differences among layers (H = 53.250; $p = 0.000$; $n = 241$). This vertical pattern of THg is common in the mineral soil of forest ecosystems, where Hg tends to vary according to soil organic C distribution with soil depth (Aastrup et al., 1991; Gong et al., 2014; Navrátil et al., 2014; Zhou et al., 2017; Gruba et al., 2019; Du et al., 2019; Ma et al., 2022). In the present study, total Hg in the mineral soil correlated positively with total organic C ($\rho = 0.757$; $p = 0.000$; $n = 241$), total N ($\rho = 0.690$; $p = 0.000$; $n = 241$) and SB ($\rho = 0.518$; $p = 0.000$; $n = 241$; Fig. 4). Therefore, soil organic matter influences THg variation in the mineral horizons of pine forest soils coinciding with that previously reported in similar studies (Obrist et al., 2009; Zhou et al., 2013; Navrátil et al., 2014, 2016). Moreover, in the same study area (NW Spain), previous research also highlighted the close relationship between THg and organic matter in A horizons of acid forest soils (Gómez-Armesto et al., 2020b, 2021a). However, the correlations of THg with total organic C, N and exchangeable base cations in the mineral soil weakened with increasing soil depth, possibly due to a diminution in organic matter content. Contrarily, metal (Al, Fe)-humus complexes and inorganic Al and Fe oxyhydroxides tended to increase with soil depth (Fig. S1). Secondary compounds of Al and Fe would provide additional binding sites for Hg immobilization, thus determining, together with organic C, the vertical Hg patterns. In this regard, THg in the whole mineral soil correlated with Fe$_p$ ($\rho = 0.300$; $p = 0.000$; $n = 241$) and Fe$_o$ ($\rho = 0.356$; $p = 0.000$; $n = 241$), also showing significant correlations with Al$_p$ and Al$_o$ at some depths (Table S5). Iron oxyhydroxides and secondary Al compounds (Al-humus complexes and inorganic non-crystalline and crystalline compounds) were reported to be actively involved in Hg retention in acid forest soils (Grimaldi et al., 2008; Guedron et al., 2009; Richardson et al., 2013; Navrátil et al., 2014, 2016; Nave et al., 2019; Gómez-Armesto et al., 2020b, 2021a, b).

On the other hand, the very low values of THg in the soil parent material (<5.2 µg kg^{-1}) and the occurrence of the highest THg levels in the uppermost mineral soil layers (0–5 and 5–10 cm) support that most
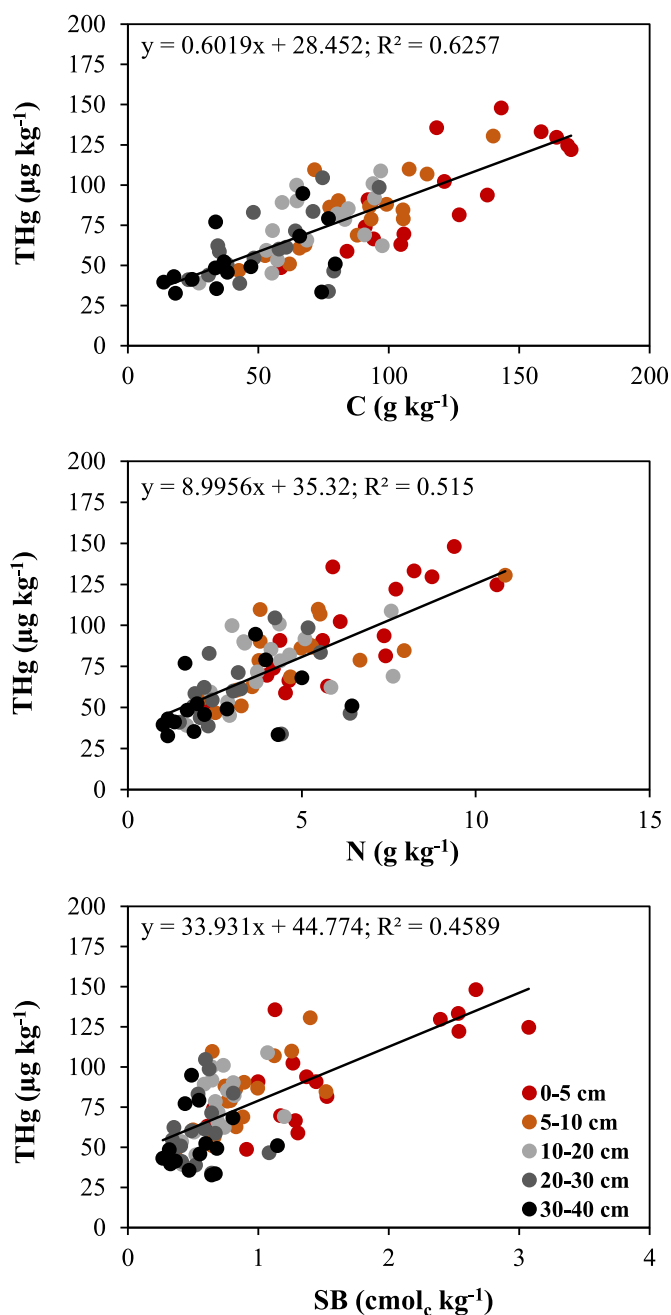
Fig. 4. Linear regression between the concentration of total Hg (THg) and total C, total N and the sum of bases (SB) in mineral soil layers.

of the Hg derived from atmospheric sources. This is consistent with studies on the isotopic Hg signature in forest soils, which revealed that more than 80% of Hg in topsoil samples comes from atmospheric deposition (Demers et al., 2013; Jiskra et al., 2015). These data for THg in the mineral soil were comparable to the range (7–161 µg kg^{-1}) reported in mineral soils under coniferous species in Central Europe (Navrátil et al., 2016; Gruba et al., 2019), the USA (Obrist et al., 2011; Blackwell et al., 2014) and China (Zhou et al., 2017).

The average Hg pool (PHg) in the whole organic horizon was 0.30 mg m^{-2} (Fig. 2), showing a greater Hg accumulation (92%) in the OF + OH subhorizon (0.28 ± 0.18 mg m^{-2}) than in the OL layer (0.03 ± 0.01 mg m^{-2}). Some characteristics of the organic horizons such as thickness, bulk density or litter age appeared to influence considerably PHg estimates (Tipping et al., 2011; Obrist et al., 2011, 2016; Navrátil et al., 2014). In the present study, the thickness and bulk density of the OF +

OH layers were significantly higher than those in the OL subhorizon (U = 495.5; p = 0.000; n = 102 and U = 321.0; p = 0.000; n = 102, respectively). This fact, together with greater THg, justifies a higher Hg storage in OF + OH than in OL subhorizons, as was already shown in previous studies (Larssen et al., 2008; Richardson and Friedland, 2015; Navrátil et al., 2016; Zhou et al., 2017). The pool of Hg (PHg) in the entire organic horizons correlated to total organic C (ρ = −0.701; p = 0.000; n = 102), total N (ρ = 0.673; p = 0.000; n = 102) and the C/N ratio (ρ = −0.732; p = 0.000; n = 102). Similar relationships between Hg pool and parameters related to soil organic matter were already evidenced in organic horizons of forest soils from the US (Obrist et al., 2009) and from different European countries (Navrátil et al., 2016; Méndez-López et al., 2022a). In summary, our results evidenced a close connection between the biogeochemical cycles of Hg and organic matter, which will determine most of the PHg in the O horizons. In addition, the mean PHg obtained in the organic horizons under *P. pinaster* were within the order of magnitude obtained in O horizons of other coniferous forest soils (Nasr and Arp, 2011; Obrist et al., 2012; Zhou et al., 2017; Du et al., 2019; Méndez-López et al., 2022a).

In the mineral soil (up to 40 cm depth), the average pool of total Hg was 22.7 mg m^{-2}, two orders of magnitude higher than the mean PHg in the organic horizons. The vertical pattern described by PHg in the mineral soil showed a steady increase up to the 10–20 cm layer (6.2 mg m^{-2}; Fig. 2) from where it slightly decreased up to 40 cm depth (5.2 mg m^{-2}). A Kruskal-Wallis test, performed with PHg values corresponding to mineral soil layers 10 cm thick, revealed that soil depth was a statistically significant variation factor for PHg (H = 10.261; p = 0.016; n = 190). Such differences of PHg values with soil depth can be attributed to unequal values of bulk density and organic matter content (Obrist et al., 2012, 2016; Gruba et al., 2019). In fact, the uppermost soil layers in the mineral soil were those with higher organic matter contents but lower bulk density, which is consistent with the inverse relationship found between both parameters in forest soils (Périé and Ouimet, 2008). In the present study, Hg stored (PHg) in the mineral soil remained closely correlated with parameters related to soil organic matter (such as C and N contents, Table S5) up to 30 cm depth. This suggests that soil ability for Hg storage in the uppermost soil layers mostly depends on the organic matter dynamics (accumulation, decomposition degree, etc), since the affinity of Hg for the reduced S groups of organic matter is well known (Skyllberg et al., 2006; He et al., 2019).

Apart from parameters related to soil organic matter, metal (Al, Fe)-humus complexes (Al$_p$, Fe$_p$) and non-crystalline Al and Fe oxyhydroxides (Al$_o$, Fe$_o$) were shown to contribute, to some extent, to PHg (Table S5). These relationships are consistent with previous studies, which already reported close correlations of C and N pools, extractable Fe and Al with PHg (Gong et al., 2014; Navrátil et al., 2014, 2016; Gómez-Armesto et al., 2021a; Chen et al., 2022). However, physical properties such as soil bulk density also influenced PHg estimates in mineral soils (Obrist et al., 2009; Panagos et al., 2021). Thus, bulk density correlated with PHg (ρ = 0.367; p = 0.000; n = 241) accounting for some of the variations found for PHg values among mineral soil layers (Fig. 2).

A reliable comparison of PHg among studies requires at least the soil thickness to be fixed (Amirbahman et al., 2004). The Hg pool in the first 20 cm of mineral soil (11.9 mg m^{-2}) was in the range of values (3–15 mg m^{-2}) described for the topsoil (i.e. 0-20 cm) in the study area (Panagos et al., 2021). Considering the whole mineral soil (up to 40 cm), the average of PHg (22.7 mg m^{-2}) was 2–4 times higher than the range of values (4–12 mg m^{-2}) reported in pine forest soils in the USA and Poland (Obrist et al., 2009; Gruba et al., 2019), where lower precipitation amounts, as well as C contents in the mineral soil, would lead to a reduced presence of Hg in the forest ecosystem, ultimately affecting PHg in the soil. The pool of Hg in the upper mineral soil layers, in addition to the Hg concentrations found in these soil layers, would be also conditioned by soil layers thickness, soil pedogenesis and organic matter turnover in the overlying OH subhorizon (Peña-Rodríguez et al., 2014;

Zheng et al., 2016). Soil pedogenesis may result in the formation of different amounts of secondary Al and Fe compounds (metal (Al, Fe)-humus complexes and inorganic crystalline and non-crystalline Al and Fe oxyhidroxides), whose distribution along the soil profile and their ability to retain Hg would explain the variations in soil Hg pools (Guedron et al., 2009; Peña-Rodríguez et al., 2012; Navrátil et al., 2016; Richardson, 2022). On the other hand, recent findings reported that a lower rate of organic matter decomposition in organic horizons of forest soils contributes to a smaller loss of Hg, favoring its accumulation (Ma et al., 2022). Estimates of soil Hg pool help to identify areas with high Hg accumulation, where land use activities should be carried out with caution in order to minimize the risks of Hg mobilization through runoff and soil erosion toward freshwater ecosystems (Panagos et al., 2021).

3.3. Variations in Hg concentration and pools along the coast-inland transect

The influence of climate on THg and PHg in pine forest soils along the coast-inland transect was examined considering the distance to the Atlantic Ocean coastline, as climatic conditions (mainly precipitation) change progressively across the study area. This change leads to defining a climatic transition from an area with a marked oceanic climate (typical of the Eurosiberian biogeographical region) to another with moderate continental features (representative of the Mediterranean biogeographical region).

The concentration of total Hg in the organic subhorizons showed a decreasing trend as pine stands were further away from the coastline (Fig. 5). In fact, a negative significant correlation was found between THg and the distance of pine stands to the coastline for OL subhorizons ($\rho = -0.552$; p = 0.000; n = 51) and OF + OH subhorizons ($\rho = -0.415$; p < 0.01; n = 51). In parallel, the mean annual precipitation for each pine stand also decreased with the distance to the coastline (Fig. S2). Therefore, a connection between THg in the organic horizons and precipitation along the study transect could be established, explaining the decline in THg for O horizons as pine stands are located further away from the coastline receiving less precipitation. This agrees with studies that pointed to precipitation as one of the main factors determining the spatial distribution of Hg in surface soil (Obrist et al., 2011, 2016; Richardson et al., 2013; Wang et al., 2019a, b; Zhang et al., 2020). Moreover, precipitation was reported to enhance net primary production, inducing in and indirect way an increased uptake of atmospheric Hg by foliar tissues (Wang et al., 2019a; Zhou and Obrist, 2021). In the study area (NW Spain), precipitation correlated to total pine needle biomass (Eimil-Fraga et al., 2015b) and THg content in pine needles (Méndez-López et al., 2022b), supporting the trend observed for THg in the O horizons of pine stands along the coast-inland transect. This

suggests that the content of Hg in the organic horizons of pine forest soils across the NW Iberian Peninsula is influenced, at a regional scale, by precipitation as a climatic driver.

Altitude is another factor influencing THg in organic horizons, with elevated environments generally showing greater Hg deposition rates due to precipitation and therefore, higher THg levels in O horizons (Szopka et al., 2011; Stankwitz et al., 2012; Blackwell and Driscoll, 2015). Conversely, THg correlated negatively with altitude in the OL subhorizon ($\rho = -0.333$; p < 0.05; n = 51) along the coast-inland transect, suggesting that Hg levels in organic horizons are more influenced by precipitation than by altitude, two parameters that showed a significant and inversely proportional relationship (p < 0.01). This is consistent with the higher Hg levels found in O horizons from pine stands close to the coastline, where altitude was usually lower than in inland stands. Moreover, as oceans are considered the largest global source of Hg to the atmosphere (Pirrone et al., 2010; Obrist et al., 2018), the organic horizons of pine stands located near the coast could receive additional loads of Hg previously scavenged from the air by tree foliage and eventually carried to soil surface through litterfall. Moreover, the removal of Hg from the atmosphere by forests near the coast could reduce the Hg burden in air masses moving away from the coast towards inland areas. This is supported by the diminution of sea-salt concentration in the air far away from the coast (Gustafsson and Franzén, 2000) that would be expected to be accompanied by a reduction in atmospheric Hg, given the strong affinity of some reactive gaseous Hg forms (RGM) for sea-salt aerosols (Malcolm et al., 2009).

The maritime influence, qualitatively determined by considering the distance to the coastline or mean annual precipitation of each pine stand, allowed discriminating THg concentrations in the organic horizons (especially in OL layers) along the coast-inland transect. As a result, pine stands belonging to the Eurosiberian region (<95 km to the coastline) showed often more THg in OL and OF + OH subhorizons than pine stands located in the Mediterranean region (Fig. 3). The climatic characteristics of the Eurosiberian region were found to be more favourable than those of the Mediterranean for *P. pinaster* productivity (Álvarez-Álvarez et al., 2011). Consequently, a greater aboveground biomass production in the pine stands from the Eurosiberian region would lead to a greater rate of Hg transference from foliar tissues to the uppermost soil layers according to that shown in Fig. 3. This is in agreement with the findings of Obrist et al. (2009) who reported, in forests from remote areas of the USA, a direct relationship between biomass productivity, higher atmospheric Hg deposition rates and greater values of C, N and Hg in soils. Therefore, climatic factors also affect THg in organic horizons at regional scales, similar to that reported by Richardson et al. (2013).

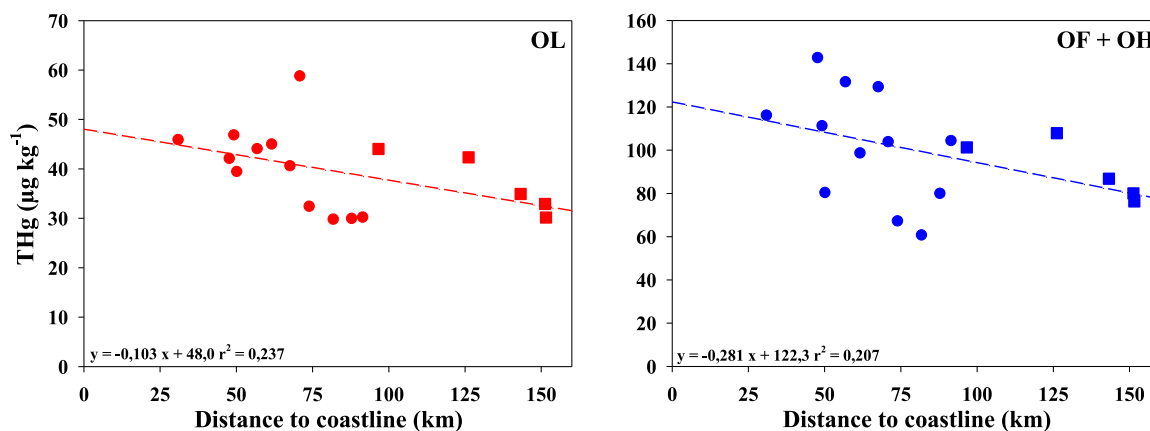In the mineral soil, only the 0–5 cm layer showed a weak but

Fig. 5. Relationship between the concentration of Hg (THg) and distance to coastline in the OL and OF + OH subhorizons of pine stands. Circles and squares indicate stands belonging to the Eurosiberian and the Mediterranean biogeographical regions, respectively.

significant correlation between THg and the distance to the coastline (ρ = -0.363; p = 0.009; n = 51) and no correlations were found between precipitation and THg in any soil layer. This suggests that, at a regional scale, climatic conditions would play a secondary role in the distribution of THg in the mineral soil, as was outlined in previous research (Obrist et al., 2011; Richardson et al., 2013). In their recent study, Ballabio et al. (2021) reported that variations in climate at larger spatial scales (i.e. at continental scale) could notably influence THg levels in the mineral topsoil (0–20 cm). The fact that the influence of the distance to the coastline on THg was restricted to the topmost mineral soil layer (0–5 cm) may be related to the biogeochemical Hg cycle in the overlying organic horizons. Therefore, changes in climatic factors along the transect would affect THg concentrations in the mineral soil indirectly, through soil components and pedogenetic processes.

The values of Hg storage (PHg) showed a slight increase with mean annual precipitation in O horizons and some mineral soil layers (Fig. S3), but there were no correlations between PHg and the distance to the coastline. This suggests that soil Hg accumulation along the coast-inland transect varied depending on post-depositional processes involving Hg interactions with soil components such as soil organic matter, pH or Al and Fe oxyhydroxides (Richardson et al., 2013). Given that soils constitute a substantial part of terrestrial ecosystems in terms of Hg storage, there is a need to assess how soil components and properties may explain THg and PHg variations in the pine forest soils distributed over the study area.

3.4. Relationships between Hg and soil properties along the coast-inland transect

Along the coast-inland transect, the C/N ratio of the organic horizons increased slightly with the distance to the coastline (Fig. S4). In accordance with this and taking into account the negative correlation found between the C/N ratio and THg, it is consistent that the lowest levels of Hg in O horizons were found in pine stands located in the Mediterranean biogeographical region (Fig. 5). The C/N ratio in the OF + OH subhorizons also decreased along the transect with increasing mean annual precipitation, suggesting that rainfall could indirectly influence THg levels by controlling organic matter dynamics, as was recently evidenced by Ma et al. (2022).

On the other hand, PHg in the organic horizons did not correlate with the distance to the coastline or precipitation, although rainfall was reported to influence Hg storage on the forest floor (Richardson et al., 2013; Blackwell et al., 2014; Wang et al., 2017, 2019b). The orography of the territory, combined with precipitation, altitude and temperature, could indirectly influence Hg pools in organic horizons through the direct effect on the rate of organic C mineralization and biomass production (Blackwell and Driscoll, 2015; Gruba et al., 2019; Wang et al., 2019b). As evidence, PHg (ρ = 0.318; p = 0.024; n = 51) and total organic C pool (ρ = 0.460; p = 0.001; n = 51) correlated with altitude in OF + OH subhorizons. This is in line with the findings reported by Ma et al. (2022), who observed that Hg concentration in the organic horizons (litter) was dependent on altitude, temperature and precipitation.

The lack of relationships among THg in the mineral soil and precipitation, altitude and distance to the coastline suggests that variations in THg along the coast-inland transect would mostly depend on the interactions between Hg and soil components (Richardson et al., 2013; Navrátil et al., 2014).

Along the coast-inland transect, PHg values in the uppermost 10 cm of the mineral soil increased with the proximity of pine stands to the coastline and with mean annual rainfall (Fig. S5). Similar trends were shown by the organic C pool, so the accumulation of Hg in the uppermost layers of the mineral soil seemed to be indirectly influenced by organic C accumulation as was reported in different studies (Szopka et al., 2011; Juillerat et al., 2012; Gruba et al., 2019; Du et al., 2019). Thus, along the transition between the Eurosiberian and the Mediterranean biogeographical regions in the NW Iberian Peninsula, the

variation in the climatic conditions (mainly precipitation) seemed to affect PHg through the accumulation of organic C. In the same study area (NW Spain), Rodríguez-Lado and Martínez-Cortizas (2015) and Calvo de Anta et al. (2020) found that precipitation was the main factor influencing soil C pool, whose highest values occurred in areas where rainfall is evenly distributed throughout the year and with short dry periods. These areas correspond to those where pine stands showed greater PHg values, most of them located in the Eurosiberian biogeographical region.

4. Conclusions

The concentration and pool of Hg varied significantly among the soil layers of the pine forests studied. The deeper organic subhorizon, i.e. OF + OH, showed the highest THg mean value, which was found to be closely correlated with the higher decomposition degree of organic matter (lower C/N ratio). In contrast, although the mineral soil layers showed lower concentrations of Hg, they appeared to be the largest reservoir of Hg, mainly due to the highest bulk density and the presence of Fe–Al compounds. The role of the mineral soil as a sink for Hg is key in its immobilization, as the deeper soil layers are not directly exposed to the effect of external disturbances such as forest management, land use changes and global warming. In addition, in pine forests that are poorly managed and therefore at high risk of wildfire, such as those studied in the present work, Hg accumulated in the mineral soil would not be expected to be released into the atmosphere.

The variation of THg along the coastal-inland transect was only observed in the uppermost soil layers (the organic horizon and the first 5 cm of mineral soil), that are directly affected by the atmospheric deposition of mercury. Thus, the forest floor is a direct receptor of atmospheric Hg, which arrives to coastal areas bound to sea salt aerosols and deposits through precipitation and fog. For this reason, together with the coastal humidity that promotes vegetative growth, there were higher concentrations of Hg in the uppermost layers of soils from pine forests close to the coast. The variation in climatic features (precipitation and temperature) and the altitude and orography of the territory could indirectly affect Hg concentrations and pools in the uppermost soil layers by controlling organic matter mineralization.

Data availability

Data will be made available on request.

Acknowledgements

Appendix A. Supplementary data

Supplementary data to this article can be found online at https://doi.org/10.1016/j.envres.2023.116155.

References

Aastrup, M., Johnson, J., Bringmark, E., Bringmark, I., Iverfeldt, Å., 1991. Occurrence and transport of mercury within a small catchment area. Water Air Soil Pollut. 56, 155–167. https://doi.org/10.1007/BF00342269.

Álvarez, E., Monterroso, C., Fernández Marcos, M.L., 2002. Aluminium fractionation in Galician (NW Spain) forest soils as related to vegetation and parent material. For. Ecol. Manage. 166, 193–206. https://doi.org/10.1016/S0378-1127(01)00658-2.

Álvarez-Álvarez, P., Khouri, E.A., Cámara-Obregón, A., Castedo-Dorado, F., Barrio-Anta, M., 2011. Effects of foliar nutrients and environmental factors on site productivity in Pinus pinaster Ait. stands in Asturias (NW Spain). Ann. For. Sci. 68, 497–509. https://doi.org/10.1007/s13595-011-0047-5.

Amirbahman, A., Ruck, P.L., Fernandez, I.J., Haines, T.A., Kahl, J.S., 2004. The effect of fire on mercury cycling in the soils of forested watersheds: Acadia National Park, Maine, U.S.A. Water. Air. Soil Pollut 152, 313–331. https://doi.org/10.1023/B:WATE.0000015369.02804.15.

Ballabio, C., Jiskra, M., Osterwalder, S., Borrelli, P., Montanarella, L., Panagos, P., 2021. A spatial assessment of mercury content in the European Union topsoil. Sci. Total Environ. 769, 144755 https://doi.org/10.1016/j.scitotenv.2020.144755.

Bishop, K., Shanley, J.B., Riscassi, A., de Wit, H.A., Eklöf, K., Meng, B., Mitchell, C., Osterwalder, S., Schuster, P.F., Webster, J., Zhu, W., 2020. Recent advances in understanding and measurement of mercury in the environment: Terrestrial Hg cycling. Sci. Total Environ. 721, 137647 https://doi.org/10.1016/j.scitotenv.2020.137647.

Blackwell, B.D., Driscoll, C.T., 2015. Deposition of mercury in forests along a montane elevation gradient. Environ. Sci. Technol. 49, 5363–5370. https://doi.org/10.1021/es505928w.

Blackwell, B.D., Driscoll, C.T., Maxwell, J.A., Holsen, T.M., 2014. Changing climate alters inputs and pathways of mercury deposition to forested ecosystems. Biogeochemistry 119, 215–228. https://doi.org/10.1007/s10533-014-9961-6.

Burns, D.A., Woodruff, L.G., Bradley, P.M., Cannon, W.F., 2014. Mercury in the soil of two contrasting watersheds in the eastern United States. PLoS One 9. https://doi.org/10.1371/journal.pone.0086855.

Calvo de Anta, R., Luís, E., Febrero-Bande, M., Galiñanes, J., Macías, F., Ortíz, R., Casás, F., 2020. Soil organic carbon in peninsular Spain: Influence of environmental factors and spatial distribution. Geoderma 370, 114365. https://doi.org/10.1016/j.geoderma.2020.114365.

Campos, I., Vale, C., Abrantes, N., Keizer, J.J., Pereira, P., 2015. Effects of wildfire on mercury mobilisation in eucalypt and pine forests. Catena 131, 149–159. https://doi.org/10.1016/j.catena.2015.02.024.

Carbone, M.S., Still, C.J., Ambrose, A.R., Dawson, T.E., Williams, A.P., Boot, C.M., Schaeffer, S.M., Schimel, J.P., 2011. Seasonal and episodic moisture controls on plant and microbial contributions to soil respiration. Oecologia 167, 265–278. https://doi.org/10.1007/s00442-011-1975-3.

Carbone, M.S., Park Williams, A., Ambrose, A.R., Boot, C.M., Bradley, E.S., Dawson, T.E., Schaeffer, S.M., Schimel, J.P., Still, C.J., 2013. Cloud shading and fog drip influence the metabolism of a coastal pine ecosystem. Global Change Biol. 19, 484–497. https://doi.org/10.1111/gcb.12054.

Chen, C., Huang, J.H., Meusburger, K., Li, K., Fu, X., Rinklebe, J., Alewell, C., Feng, X., 2022. The interplay between atmospheric deposition and soil dynamics of mercury in Swiss and Chinese boreal forests: A comparison study. Environ. Pollut. 307, 119483 https://doi.org/10.1016/j.envpol.2022.119483.

Cheng, I., Zhang, L., Blanchard, P., Dalziel, J., Tordon, R., Huang, J., Holsen, T.M., 2013. Comparisons of mercury sources and atmospheric mercury processes between a coastal and inland site. J. Geophys. Res. Atmos. 118, 2434–2443. https://doi.org/10.1002/jgrd.50169.

Coale, K.H., Heim, W.A., Negrey, J., Weiss-Penzias, P., Fernandez, D., Olson, A., Chiswell, H., Byington, A., Bonnema, A., Martenuk, S., 2018. The distribution and speciation of mercury in the California current: Implications for mercury transport via fog to land. Deep Sea Res. Part II Top. Stud. Oceanogr. 151, 77–88. https://doi.org/10.1016/j.dsr2.2018.05.012.

Cools, N., Vesterdal, L., De Vos, B., Vanguelova, E., Hansen, K., 2014. Tree species is the major factor explaining C: N ratios in European forest soils. For. Ecol. Manage. 311, 3–16. https://doi.org/10.1016/j.foreco.2013.06.047.

Demers, J.D., Driscoll, C.T., Fahey, T.J., Yavitt, J.B., 2007. Mercury cycling in litter and soil in different forest types in the Adirondack region, New York, USA. Ecol. Appl. 17, 1341–1351. https://doi.org/10.1890/06-1697.1.

Demers, J.D., Blum, J.D., Zak, D.R., 2013. Mercury isotopes in a forested ecosystem: Implications for air-surface exchange dynamics and the global mercury cycle. Global Biogeochem. Cycles 27, 222–238. https://doi.org/10.1002/gbc.20021.

de Diego, J., Rúa, A., Fernández, M., 2021. Vulnerability variables and their effect on wildfires in galicia (Spain). a panel data analysis. Land 10, 1004. https://doi.org/10.3390/land10101004.

Du, B., Zhou, J., Zhou, L., Fan, X., Zhou, J., 2019. Mercury distribution in the foliage and soil profiles of a subtropical forest: Process for mercury retention in soils. J. Geochem. Explor. 205, 106337 https://doi.org/10.1016/j.gexplo.2019.106337.

Eckley, C.S., Eagles-Smith, C., Tate, M.T., Kowalski, B., Danehy, R., Johnson, S.L., Krabbenhoft, D.P., 2018. Stream Mercury Export in Response to Contemporary Timber Harvesting Methods (Pacific Coastal Mountains, Oregon, USA). Environ. Sci. Technol. 52, 1971–1980. https://doi.org/10.1021/acs.est.7b05197.

Eimil-Fraga, C., Álvarez-Rodríguez, E., Rodríguez-Soalleiro, R., Fernández-Sanjurjo, M. J., 2015a. The influence of parent material on the aluminium fractions in acidic soils under Pinus pinaster in Galicia (NW Spain). Geoderma 255–256, 50–57. https://doi.org/10.1016/j.geoderma.2015.04.026.

Eimil-Fraga, C., Sánchez-Rodríguez, F., Álvarez-Rodríguez, E., Rodríguez-Soalleiro, R., 2015b. Relationships between needle traits, needle age and site and stand parameters in Pinus pinaster. Trees (Berl.) 29, 1103–1113. https://doi.org/10.1007/s00468-015-1190-7.

Ferro-Vázquez, C., Nóvoa-Muñoz, J.C., Costa-Casais, M., Klaminder, J., Martínez-Cortizas, A., 2014. Metal and organic matter immobilization in temperate podzols: A high resolution study. Geoderma 217–218. https://doi.org/10.1016/j.geoderma.2013.10.006.

Fischer, D.T., Still, C.J., Ebert, C.M., Baguskas, S.A., Williams, A.P., 2016. Fog drip maintains dry season ecological function in a California coastal pine forest. Ecosphere 7, e01364. https://doi.org/10.1002/ecs2.1364.

Fonseca, F., De Figueiredo, T., 2018. Carbon and nitrogen in forest floor and mineral soil under four forest species in the Mediterranean region. Spanish J. Soil Sci. 8, 42–56. https://doi.org/10.3232/SJSS.2018.V8.N1.04.

gal, Meteogalicia, 2022. Meteogalicia. Concellería de Medio Ambiente. Territorio e Vivenda. Xunta de Galicia. https://www.meteogalicia.gal.

Gómez-Armesto, A., Méndez-López, M., Pérez-Rodríguez, P., Fernández-Calviño, D., Arias-Estévez, M., Nóvoa-Muñoz, J.C., 2020a. Litterfall Hg deposition to an oak forest soil from southwestern Europe. J. Environ. Manag. 269, 110858 https://doi.org/10.1016/j.jenvman.2020.110858.

Gómez-Armesto, A., Martínez-Cortizas, A., Ferro-Vázquez, C., Méndez-López, M., Arias-Estévez, M., Nóvoa-Muñoz, J.C., 2020b. Modelling Hg mobility in podzols: Role of soil components and environmental implications. Environ. Pollut. 260, 114040 https://doi.org/10.1016/j.envpol.2020.114040.

Gómez-Armesto, A., Méndez-López, M., Pontevedra-Pombal, X., García-Rodeja, E., Alonso-Vega, F., Arias-Estévez, M., Nóvoa-Muñoz, J.C., 2021a. Soil properties influencing Hg vertical pattern in temperate forest podzols. Environ. Res. 193, 110552 https://doi.org/10.1016/j.envres.2020.110552.

Gómez-Armesto, A., Méndez-López, M., Marques, P., Pontevedra-Pombal, X., Monteiro, F., Madeira, M., Arias-Estévez, M., Nóvoa-Muñoz, J.C., 2021b. Patterning total mercury distribution in coastal podzolic soils from an Atlantic area: Influence of pedogenetic processes and soil components. Catena 206, 105540. https://doi.org/10.1016/j.catena.2021.105540.

Gong, P., Wang, X.P., Xue, Y.G., Xu, B.Q., Yao, T.D., 2014. Mercury distribution in the foliage and soil profiles of the Tibetan forest: Processes and implications for regional cycling. Environ. Pollut. 188, 94–101. https://doi.org/10.1016/j.envpol.2014.01.020.

Grigal, D.F., 2003. Mercury sequestration in forests and peatlands: A review. J. Environ. Qual. 32, 393–405. https://doi.org/10.2134/jeq2003.0393.

Grimaldi, C., Grimaldi, M., Guedron, S., 2008. Mercury distribution in tropical soil profiles related to origin of mercury and soil processes. Sci. Total Environ. 401, 121–129. https://doi.org/10.1016/j.scitotenv.2008.04.001.

Gruba, P., Socha, J., Pietrzykowski, M., Pasychnyk, D., 2019. Tree species affects the concentration of total mercury (Hg) in forest soils: Evidence from a forest soil inventory in Poland. Sci. Total Environ. 647, 141–148. https://doi.org/10.1016/j.scitotenv.2018.07.452.

Guedron, S., Grangeon, S., Lanson, B., Grimaldi, M., 2009. Mercury speciation in a tropical soil association; Consequence of gold mining on Hg distribution in French Guiana. Geoderma 153, 331–346. https://doi.org/10.1016/j.geoderma.2009.08.017.

Gustafsson, M.E., Franzén, L.G., 2000. Inland transport of marine aerosols in southern Sweden. Atmos. Environ. 34 (2), 313–325. https://doi.org/10.1016/S1352-2310(99)00198-3.

Gustin, M.S., Lindberg, S.E., Weisberg, P.J., 2008. An update on the natural sources and sinks of atmospheric mercury. Appl. Geochem. 23, 482–493. https://doi.org/10.1016/j.apgeochem.2007.12.010.

Hagen-Thorn, A., Callesen, I., Armolaitis, K., Nihlgård, B., 2004. The impact of six European tree species on the chemistry of mineral topsoil in forest plantations on former agricultural land. For. Ecol. Manage. 195, 373–384. https://doi.org/10.1016/j.foreco.2004.02.036.

He, M., Tian, L., Braaten, H.F.V., Wu, Q., Luo, J., Cai, L.M., Meng, J.H., Lin, Y., 2019. Mercury–Organic Matter Interactions in Soils and Sediments: Angel or Devil? Bull. Environ. Contam. Toxicol. 102, 621–627. https://doi.org/10.1007/s00128-018-2523-1.

Herrero, C., Turrión, M.B., Pando, V., Bravo, F., 2016. Carbon content of forest floor and mineral soil in Mediterranean Pinus spp. and Oak stands in acid soils in Northern Spain. For. Syst. 25 https://doi.org/10.5424/fs/2016252-09149.

Jiskra, M., Wiederhold, J.G., Skyllberg, U., Kronberg, R.-M., Hajdas, I., Kretzschmar, R., 2015. Mercury deposition and re-emission pathways in boreal forest soils investigated with Hg isotope signatures. Environ. Sci. Technol. 49, 7188–7196. https://doi.org/10.1021/acs.est.5b00742.

Jiskra, M, Sonke, J.E., Obrist, D., Bieser, J., Ebinghaus, R., Myhre, C.L., Pfaffhuber, K.A., Wängberg, I., Kyllönen, K., Worthy, D., Martin, L.G., Labuschagne, C., Mkololo, T., Ramonet, M., Magand, O., Dommergue, A., 2018. A vegetation control on seasonal variations in global atmospheric mercury concentrations. Nat. Geosci. 11, 244–250. https://doi.org/10.1038/s41561-018-0078-8.

Juillerat, J.I., Ross, D.S., Bank, M.S., 2012. Mercury in litterfall and upper soil horizons in forested ecosystems in Vermont, USA. Environ. Toxicol. Chem. 31, 1720–1729. https://doi.org/10.1002/etc.1896.

Kaal, J., Costa-Casais, M., Ferro-Vázquez, C., Pontevedra-Pombal, X., Martínez-Cortizas, A., 2008. Soil Formation of "Atlantic Rankers" from NW Spain - A High Resolution Aluminium and Iron Fractionation Study. Pedosphere 18, 441–453. https://doi.org/10.1016/S1002-0160(08)60035-1.

Kumar, A., Wu, S., Huang, Y., Liao, H., Kaplan, J.O., 2018. Mercury from wildfires: Global emission inventories and sensitivity to 2000–2050 global change. Atmos. Environ. 173, 6–15. https://doi.org/10.1016/j.atmosenv.2017.10.061.

Larssen, T., de Wit, H.A., Wiker, M., Halse, K., 2008. Mercury budget of a small forested boreal catchment in southeast Norway. Sci. Total Environ. 404, 290–296. https://doi.org/10.1016/j.scitotenv.2008.03.013.

López-Marcos, D., Martínez-Ruiz, C., Turrión, M.-B., Jonard, M., Titeux, H., Ponette, Q., Bravo, F., 2018. Soil carbon stocks and exchangeable cations in monospecific and mixed pine forests. Eur. J. For. Res. 137, 831–847. https://doi.org/10.1007/s10342-018-1143-y.

Louis, V.L.S.T., Rudd, J.W.M., Kelly, C.A., Hall, B.D., Rolfhus, K.R., Scott, K.J., Lindberg, S.E., Dong, W., 2001. Importance of the forest canopy to fluxes of methyl mercury and total mercury to boreal ecosystems. Environ. Sci. Technol. 35, 3089–3098. https://doi.org/10.1021/es001924p.

Ma, H., Cheng, H., Guo, F., Zhang, L., Tang, S., Yang, Z., Peng, M., 2022. Distribution of mercury in foliage, litter and soil profiles in forests of the Qinling Mountains, China. Environ. Res. 211, 113017 https://doi.org/10.1016/j.envres.2022.113017.

Malcolm, E.G., Ford, A.C., Redding, T.A., Richardson, M.C., Strain, B.M., Tetzner, S.W., 2009. Experimental investigation of the scavenging of gaseous mercury by sea salt aerosol. J. Atmos. Chem. 63, 221–234. https://doi.org/10.1007/s10874-010-9165-y.

Martí-Ezpeleta, A., Cuadrat-Prats, J.M., Marzol-Jaén, M.V., Ollero-Ojeda, A., Sánchez-Fabre, M., 2018. Clima y agua. In: Serie Compendios del Atlas Nacional de España (ANE). Centro Nacional de Información Geográfica, pp. 92–114. https://www.ign.es/web/resources/docs/IGNCnig/ANE/Capitulos/04_Climayagua.pdf.

Martínez-Cortizas, A., Castillo-Rodríguez, F., Blanco-Chao, R., 1999. Precipitación. In: Martínez-Cortizas, A., Pérez-Alberti, A. (Eds.), Atlas Climático de Galicia, Xunta de Galicia, pp. 75–93. Santiago de Compostela.

Méndez-López, M., Gómez-Armesto, A., Alonso-Vega, F., Pontevedra-Pombal, X., Fonseca, F., de Figueiredo, T., Arias-Estévez, M., Nóvoa-Muñoz, J.C., 2022a. The role of afforestation species as a driver of Hg accumulation in organic horizons of forest soils from a Mediterranean mountain area in SW Europe. Sci. Total Environ. 827, 154345 https://doi.org/10.1016/j.scitotenv.2022.154345.

Méndez-López, M., Gómez-Armesto, A., Eimil-Fraga, C., Alonso-Vega, F., Rodríguez-Soalleiro, R., Álvarez-Rodríguez, E., Arias-Estévez, M., Nóvoa-Muñoz, J.C., 2022b. Needle age and precipitation as drivers of Hg accumulation and deposition in coniferous forests from a southwestern European Atlantic region. Environ. Res. 215, 114223 https://doi.org/10.1016/j.envres.2022.114223.

Nasr, M., Arp, P.A., 2011. Hg concentrations and accumulations in fungal fruiting bodies, as influenced by forest soil substrates and moss carpets. Appl. Geochem. 26, 1905–1917. https://doi.org/10.1016/j.apgeochem.2011.06.014.

Nave, L.E., Covarrubias Ornelas, A., Drevnick, P.E., Gallo, A., Hatten, J.A., Heckman, K. A., Matosziuk, L., Sanclements, M., Strahm, B.D., Veverica, T.J., Weiglein, T.L., Swanston, C.W., 2019. Carbon–Mercury Interactions in Spodosols Assessed through Density Fractionation, Radiocarbon Analysis, and Soil Survey Information. Soil Sci. Soc. Am. J. 83, 190–202. https://doi.org/10.2136/sssaj2018.06.0227.

Navrátil, T., Shanley, J., Rohovec, J., Hojdová, M., Penížek, V., Buchtová, J., 2014. Distribution and pools of mercury in Czech forest soils. Water. Air. Soil Pollut 225, 1829. https://doi.org/10.1007/s11270-013-1829-1.

Navrátil, T., Shanley, J.B., Rohovec, J., Oulehle, F., Šimecek, M., Houška, J., Cudlín, P., 2016. Soil mercury distribution in adjacent coniferous and deciduous stands highly impacted by acid rain in the Ore Mountains, Czech Republic. Appl. Geochem. 75, 63–75. https://doi.org/10.1016/j.apgeochem.2016.10.005.

Obrist, D., Johnson, D.W., Lindberg, S.E., 2009. Mercury concentrations and pools in four sierra nevada forest sites, and relationships to organic carbon and nitrogen. Biogeosciences 6 (5), 765–777. https://doi.org/10.5194/bg-6-765-2009.

Obrist, D., Johnson, D.W., Lindberg, S.E., Luo, Y., Hararuk, O., Bracho, R., Battles, J.J., Dail, D.B., Edmonds, R.L., Monson, R.K., Ollinger, S.V., Pallardy, S.G., Pregitzer, K. S., Todd, D.E., 2011. Mercury distribution across 14 U.S. Forests. Part I: Spatial patterns of concentrations in biomass, litter, and soils. Environ. Sci. Technol. 45, 3974–3981. https://doi.org/10.1021/es104384m.

Obrist, D., Johnson, D.W., Edmonds, R.L., 2012. Effects of vegetation type on mercury concentrations and pools in two adjacent coniferous and deciduous forests. J. Plant Nutr. Soil Sci. 175, 68–77. https://doi.org/10.1002/jpln.201000415.

Obrist, D., Pearson, C., Webster, J., Kane, T., Lin, C.-J., Aiken, G.R., Alpers, C.N., 2016. A synthesis of terrestrial mercury in the western United States: Spatial distribution defined by land cover and plant productivity. Sci. Total Environ. 568, 522–535. https://doi.org/10.1016/j.scitotenv.2015.11.104.

Obrist, D., Kirk, J.L., Zhang, L., Sunderland, E.M., Jiskra, M., Selin, N.E., 2018. A review of global environmental mercury processes in response to human and natural perturbations: Changes of emissions, climate, and land use. Ambio 47, 116–140. https://doi.org/10.1007/s13280-017-1004-9.

Obrist, D., Roy, E.M., Harrison, J.L., Kwong, C.F., William Munger, J., Moosmüller, H., Romero, C.D., Sun, S., Zhou, J., Commane, R., 2021. Previously unaccounted atmospheric mercury deposition in a midlatitude deciduous forest. Proc. Natl. Acad. Sci. U. S. A 118, e2105477118. https://doi.org/10.1073/pnas.2105477118.

Panagos, P., Jiskra, M., Borrelli, P., Liakos, L., Ballabio, C., 2021. Mercury in European topsoils: Anthropogenic sources, stocks and fluxes. Environ. Res. 201, 111556 https://doi.org/10.1016/j.envres.2021.111556.

Peña-Rodríguez, S., Fernández-Calviño, D., Taboada, T., Arias-Estévez, M., Martínez-Cortizas, A., Nóvoa-Muñoz, J.C., García-Rodeja, E., 2012. Mercury content in volcanic soils across Europe and its relationship with soil properties. J. Soils Sediments 12, 542–555. https://doi.org/10.1007/s11368-011-0468-7.

Peña-Rodríguez, S., Pontevedra-Pombal, X., Gayoso, E.G.R., Moretto, A., Mansilla, R., Cutillas-Barreiro, L., Arias-Estévez, M., Nóvoa-Muñoz, J.C., 2014. Mercury distribution in a toposequence of sub-Antarctic forest soils of Tierra del Fuego (Argentina) as consequence of the prevailing soil processes. Geoderma 232–234, 130–140. https://doi.org/10.1016/j.geoderma.2014.04.040.

Périé, C., Ouimet, R., 2008. Organic carbon, organic matter and bulk density relationships in boreal forest soils. Can. J. Soil Sci. 88, 315–325. https://doi.org/10.4141/CJSS06008.

Pirrone, N., Cinnirella, S., Feng, X., Finkelman, R.B., Friedli, H.R., Leaner, J., Mason, R., Mukherjee, A.B., Stracher, G.B., Streets, D.G., Telmer, K., 2010. Global mercury emissions to the atmosphere from anthropogenic and natural sources. Atmos. Chem. Phys. 10, 5951–5964. https://doi.org/10.5194/acp-10-5951-2010.

Pleijel, H., Klingberg, J., Nerentorp, M., Broberg, M.C., Nyirambangutse, B., Munthe, J., Wallin, G., 2021. Mercury accumulation in leaves of different plant types-the significance of tissue age and specific leaf area. Biogeosciences 18, 6313–6328. https://doi.org/10.5194/bg-18-6313-2021.

Pokharel, A.K., Obrist, D., 2011. Fate of mercury in tree litter during decomposition. Biogeosciences 8, 2507–2521. https://doi.org/10.5194/bg-8-2507-2011.

Porvari, P., Verta, M., Munthe, J., Haapanen, M., 2003. Forestry practices increase mercury and methyl mercury output from boreal forest catchments. Environ. Sci. Technol. 37, 2389–2393. https://doi.org/10.1021/es0340174.

Richardson, J.B., 2022. Shale weathering profiles show Hg sequestration along a New York–Tennessee transect. Environ. Geochem. Health 44 (10), 3515–3526. https://doi.org/10.1007/s10653-021-01110-x.

Richardson, J.B., Friedland, A.J., 2015. Mercury in coniferous and deciduous upland forests in northern New England, USA: Implications of climate change. Biogeosciences 12, 6737–6749. https://doi.org/10.5194/bg-12-6737-2015.

Richardson, J.B., Friedland, A.J., Engerbretson, T.R., Kaste, J.M., Jackson, B.P., 2013. Spatial and vertical distribution of mercury in upland forest soils across the northeastern United States. Environ. Pollut. 182, 127–134. https://doi.org/10.1016/j.envpol.2013.07.011.

Rodríguez-Lado, L., Martínez-Cortizas, A., 2015. Modelling and mapping organic carbon content of topsoils in an Atlantic area of southwestern Europe (Galicia, NW-Spain). Geoderma 245–246, 65–73. https://doi.org/10.1016/j.geoderma.2015.01.015.

Skyllberg, U., 2010. Mercury Biogeochemistry in Soils and Sediments, Developments in Soil Science.

Skyllberg, U., Bloom, P.R., Qian, J., Lin, C.-M., Bleam, W.F., 2006. Complexation of mercury(II) in soil organic matter: EXAFS evidence for linear two-coordination with reduced sulfur groups. Environ. Sci. Technol. 40, 4174–4180. https://doi.org/10.1021/es0600577.

Stankwitz, C., Kaste, J.M., Friedland, A.J., 2012. Threshold increases in soil lead and mercury from tropospheric deposition across an elevational gradient. Environ. Sci. Technol. 46, 8061–8068. https://doi.org/10.1021/es204208w.

Szopka, K., Karczewska, A., Kabała, C., 2011. Mercury accumulation in the surface layers of mountain soils: A case study from the Karkonosze Mountains, Poland. Chemosphere 83, 1507–1512. https://doi.org/10.1016/j.chemosphere.2011.01.049.

Tipping, E., Poskitt, J.M., Lawlor, A.J., Wadsworth, R.A., Norris, D.A., Hall, J.R., 2011. Mercury in United Kingdom topsoils; Concentrations, pools, and Critical Limit exceedances. Environ. Pollut. 159, 3721–3729. https://doi.org/10.1016/j.envpol.2011.07.011.

Tsyro, S., Aas, W., Soares, J., Sofiev, M., Berge, H., Spindler, G., 2011. Modelling of sea salt concentrations over Europe: Key uncertainties and comparison with observations. Atmos. Chem. Phys. 11, 10367–10388. https://doi.org/10.5194/acp-11-10367-2011.

Un Environment, 2019. Global Mercury Assessment 2018. UN Environment Programme Chemicals and Health Branch, Geneva, Switzerland.

Wang, X., Bao, Z., Lin, C.-J., Yuan, W., Feng, X., 2016. Assessment of Global Mercury Deposition through Litterfall. Environ. Sci. Technol. 50, 8548–8557. https://doi.org/10.1021/acs.est.5b06351.

Wang, X., Luo, J., Yin, R., Yuan, W., Lin, C.-J., Sommar, J., Feng, X., Wang, H., Lin, C., 2017. Using mercury isotopes to understand mercury accumulation in the montane

forest floor of the Eastern Tibetan Plateau. Environ. Sci. Technol. 51, 801–809. https://doi.org/10.1021/acs.est.6b03806.

Wang, Xun, Yuan, W., Lin, C.-J., Zhang, L., Zhang, H., Feng, X., 2019a. Climate and vegetation as primary drivers for global mercury storage in surface soil. Environ. Sci. Technol. 53, 10665–10675. https://doi.org/10.1021/acs.est.9b02386.

Wang, X., Yuan, W., Lu, Z., Lin, C.-J., Yin, R., Li, F., Feng, X., 2019b. Effects of Precipitation on Mercury Accumulation on Subtropical Montane Forest Floor: Implications on Climate Forcing. J. Geophys. Res. Biogeosciences 124 (4), 959–972. https://doi.org/10.1029/2018JG004809.

Wright, L.P., Zhang, L., Marsik, F.J., 2016. Overview of mercury dry deposition, litterfall, and throughfall studies. Atmos. Chem. Phys. 16, 13399–13416. https://doi.org/10.5194/acp-16-13399-2016.

Yuan, W., Wang, X., Lin, C.J., Zhang, H., Feng, X., Lu, Z., 2022. Impacts of Extreme Weather on Mercury Uptake and Storage in Subtropical Forest Ecosystems. J. Geophys. Res. Biogeosciences 127, e2021JG006681. https://doi.org/10.1029/2021JG006681.

Zanella, A., Ponge, J., Jabiol, B., Sartori, G., Kolb, E., Gobat, J., Bayon, R.L., Aubert, M., Waal, R.D., Delft, B.V., Vacca, A., Serra, G., Chersich, S., Andreetta, A., Cools, N., Englisch, M., Hager, H., Katzensteiner, K., Brêthes, A., Nicola, C.D., Testi, A., Bernier, N., Graefe, U., Juilleret, J., Banas, D., Garlato, A., Obber, S., Galvan, P., Zampedri, R., Frizzera, L., Tomasi, M., Menardi, R., Fontanella, F., Filoso, C., Dibona, R., Bolzonella, C., Pizzeghello, D., Carletti, P., Langohr, R., Cattaneo, D.,

Nardi, S., Nicolini, G., Viola, F., 2018. Humusica 1, article 4: terrestrial humus systems and forms — specific terms and diagnostic horizons. Appl. Soil Ecol. 122, 56–74. https://doi.org/10.1016/j.apsoil.2017.07.005.

Zhang, Z.Y., Li, G., Yang, L., Wang, X.J., Sun, G.X., 2020. Mercury distribution in the surface soil of China is potentially driven by precipitation, vegetation cover and organic matter. Environ. Sci. Eur. 32 https://doi.org/10.1186/s12302-020-00370-1.

Zheng, W., Obrist, D., Weis, D., Bergquist, B.A., 2016. Mercury isotope compositions across North American forests. Global Biogeochem. Cycles 30, 1475–1492. https://doi.org/10.1002/2015GB005323.

Zhou, J., Feng, X., Liu, H., Zhang, H., Fu, X., Bao, Z., Wang, X., Zhang, Y., 2013. Examination of total mercury inputs by precipitation and litterfall in a remote upland forest of Southwestern China. Atmos. Environ. 81, 364–372. https://doi.org/10.1016/j.atmosenv.2013.09.010.

Zhou, J., Wang, Z., Zhang, X., Gao, Y., 2017. Mercury concentrations and pools in four adjacent coniferous and deciduous upland forests in Beijing, China. J. Geophys. Res. Biogeosciences 122, 1260–1274. https://doi.org/10.1002/2017JG003776.

Zhou, J., Obrist, D., 2021. Global mercury assimilation by vegetation. Environ. Sci. Technol. 55 (20), 14245–14257.

Zhou, J., Obrist, D., Dastoor, A., Jiskra, M., Ryjkov, A., 2021. Vegetation uptake of mercury and impacts on global cycling. Nat. Rev. Earth Environ. 2, 269–284. https://doi.org/10.1038/s43017-021-00146-y.